Dynamin: Possible Mechanism of "Pinchase" Action

Michael M. Kozlov
Department of Physiology and Pharmacology, Sackler Faculty of Medicine, Tel Aviv University, Ramat Aviv, Tel Aviv 69978, Israel

ABSTRACT Dynamin is a GTPase playing an essential role in ubiquitous intra cellular processes involving separation of vesicles from plasma membranes and membranes of cellular compartments. Recent experimental progress (Sweitzer and Hinshaw, 1998. *Cell*. 93:1021–1029; Takei et al., 1998. *Cell.* 94:131–141) has made it possible to attempt to understand the action of dynamin in physical terms. Dynamin molecules are shown to bind to a lipid membrane, to self-assemble into a helicoidal structure constricting the membrane into a tubule, and, as a result of GTP hydrolysis, to mediate fission of this tubule (Sweitzer and Hinshaw, 1998). In a similar way, dynamin is supposed to mediate fission of a neck connecting an endocytic bud and the plasma membrane, i.e., to complete endocytosis. We suggest a mechanism of this "pinchase" action of dynamin. We propose that, as a result of GTP hydrolysis, dynamin undergoes a conformational change manifested in growth of the pitch of the dynamin helix. We show that this gives rise to a dramatic change of shape of the tubular membrane constricted inside the helix, resulting in a local tightening of the tubule, which is supposed to promote its fission. We treat this model in terms of competing elasticities of the dynamin helix and the tubular membrane and discuss the predictions of the model in relation to the previous views on the mechanism of dynamin action.

INTRODUCTION

Recently, a breakthrough has been reached in studies of membranes coated by dynamin, a 100-kDa member of the GTPase family (Sweitzer and Hinshaw, 1998; Takei et al., 1998). The level of phenomenological knowledge on these systems became sufficient to start thinking about the physics of their structural transformations (McNiven, 1998; Sweitzer and Hinshaw, 1998). The goal of the present work is to suggest a specific mechanism underlying one of the most striking and biologically important actions of dynamin: transformation of membrane tubules into vesicles (Sweitzer and Hinshaw, 1998).

As several extensive and informative reviews on dynamin have appeared recently (McNiven, 1998; Schmid et al., 1998; Kirchhausen, 1998), we only sketch here the major facts, giving a necessary basis for the present study.

Dynamin plays an essential role in numerous intracellular events involving formation of vesicles from the plasma membranes and the membranes of cellular compartments; these include calveolae internalization (Henley et al., 1998; Oh et al., 1998), budding from the Golgi complex (Jones et al., 1998), clathrin-mediated endocytosis, and synaptic vesicle recycling (see, for reviews, Warnock and Schmid, 1996; Urrutia et al., 1997; Schmid et al., 1998). The two latter processes are better investigated than the others and served as a basis for the following working scheme of dynamin action (Sweitzer and Hinshaw, 1998; Schmid et al., 1998). Initially, dynamin exists as an elongated molecule consisting of four 100K polypeptides (Hinshaw and Schmid, 1995). At some stage of endocytosis, the dynamin molecules are targeted to a budding vesicle, which is still connected to the plasma membrane by a membrane neck. Dynamin self-assembles at the vesicle neck into a multimer of a spiral shape and forms a helical collar around the neck. At a following stage, dynamin hydrolyzes bound GTP and undergoes a conformational change, resulting in fission of the neck and separation of the vesicle from the plasma membrane, i.e., it acts as a "pinchase."

The experimental studies that gave rise to this model may be divided into two stages. An extensive work of many groups produced indirect but strong support for formation of the helical collars about the necks of the vesicles (see, for review, McNiven, 1998; Schmid et al., 1998). We mention below only a few of these studies. On one hand, investigations of the nerve terminals of mutant *shibire*^{ts} flies by thin-section electron microscopy (Kosaka and Ikeda, 1983) revealed electron-dense "collars" around the necks of coated pits. On the other hand, Hinshaw and Schmid (1995) have demonstrated that dynamin molecules self-assemble in aqueous solution into spirals, provided that specific conditions are reached (Hinshaw and Schmid, 1995; Carr and Hinshaw, 1997). And, finally, Takei et al. (1995) have shown that incubation of specific membranes (hypothonically lysed rat brain synaptosomes) in brain cytosol and $GTP_{\gamma}S$ results in formation of tubular invaginations decorated by dynamin ring-like structures. The dynamin spirals in aqueous solution (Hinshaw and Schmid, 1995) and the dynamin-coated tubular invaginations (Takei et al., 1995) had the same diameter of (~50 nm) as the proteinic structures seen at the necks of coated pits (Kosaka and Ikeda, 1983). Thus a conclusion has been made that in all of these systems dynamin formed similar spirals. In the cases of "collars" of coated pits (Kosaka and Ikeda, 1983) and invaginations of synaptosomal membranes (Takei et al.,

Received for publication 5 January 1999 and in final form 31 March 1999.
Address reprint requests to Dr. Michael M. Kozlov, Department of Physiology and Pharmacology, Sackler Faculty of Medicine, Tel Aviv University, Ramat Aviv, Tel Aviv 69978, Israel. Tel.: 972-3-640-7863; Fax: 972-3-640-9113; E-mail: misha@picard.tau.ac.il.

0006-3495/99/07/604/13 $2.00

1995), these dynamin helices constricted the membrane tubules inside them.

However, the "pinchase" function of dynamin driving the final step of endocytosis remained purely hypothetical. Moreover, relating to such a complex biological process as endocytosis one would expect a priori that the mechanism of dynamin action at each stage of the presented scheme is sophisticated and involves an interplay between dynamin and other molecules such as specific synaptic membrane proteins, clathrin, and various cytosolic proteins (Takei et al., 1998, and references therein).

The second stage in the investigations of the role of dynamin can be related to a novel assay reported by Sweitzer and Hinshaw (1998) together with a recent investigation by Takei et al. (1998). These studies demonstrated that the mechanism by which dynamin is involved in the process of endocytosis may be rather simple and nonspecific. Moreover, the work by Sweitzer and Hinshaw (1998) provided experimental evidence of the "pinchase" action of dynamin.

It has been demonstrated that brain cytosol induces formation of dynamin-coated tubules not only from synaptic membranes, but also from membranes, such as inside-out erythrocyte vesicles (Takei et al., 1998) and liposomes of several lipid compositions (Sweitzer and Hinshaw, 1998; Takei et al., 1998), which do not have any endocytic function and, hence, do not contain any specific intrinsic proteins. Dynamin-mediated tubulation was even more prominent in liposomes than in synaptic membranes (Takei et al., 1998), provided that the composition of the liposomes was favorable for dynamin recruitment. Further studies on liposomes showed that the membrane tubulation by dynamin does not require nucleotides and cytosolic proteins (Sweitzer and Hinshaw, 1998; Takei et al., 1998). Thus constriction by dynamin of initially flat membranes into tubules requires for its realization just purified dynamin and lipid membranes of a suitable composition. Analysis of electron micrographs of the dynamin-coated lipid tubules revealed (Sweitzer and Hinshaw, 1998) that dynamin was bound to the lipid in a well-ordered helical lattice with a repeat distance of 132 Å. The external diameter of the dynamin helix was ~50 nm, and the diameter of the lipid tubules constricted by the helix was ~30 nm.

An essential novel finding (Sweitzer and Hinshaw, 1998) was that treatment of the dynamin-coated tubules with 1 mM GTP followed by GTP hydrolysis resulted in rapid fission of the tubules and formation of numerous dynamin-coated vesicles with a consistent diameter of 60 ∓ 20 nm. This is a direct observation of the "pinchase" action of dynamin, on one hand, and, on the other, a demonstration that hydrolysis of bound GTP is the factor causing the fission. The few tubules remaining after GTP treatment were twisted, and their external diameter was reduced to ~40 nm.

The results of Sweitzer and Hinshaw (1998) and Takei et al. (1998) reduce an a priori complex system to one consisting of only two interacting components, dynamin and lipid bilayer. They drastically limit the possible speculations about the mechanisms driving the system and, hence, provide a basis for its analysis in terms of physics. Initial hypotheses on physical mechanisms of dynamin action have been formulated by Sweitzer and Hinshaw (1998) and McNiven (1998). It was suggested that upon binding of dynamin directly to the lipid bilayer, interaction between the dynamin molecules drives their self-assembly into spirals (McNiven, 1998), accompanied by constriction of the bilayer into a tubule (Sweitzer and Hinshaw, 1998; McNiven, 1998). Hydrolysis of bound GTP was proposed to result in a conformational change of dynamin manifested in further constriction of the spiral. Severing of the membrane tubule is suggested to result from this additional constriction of the dynamin helix (Sweitzer and Hinshaw, 1998; McNiven, 1998).

The present study suggests a specific mechanism of fission of a membrane tubule by dynamin different from the mechanisms proposed previously. Our model is motivated by the observation that the diameter of the dynamin-coated vesicles resulting from fission of the tubules and supposed to represent the final configuration of dynamin after GTP hydrolysis is ~60 nm. This is practically equal to or even slightly larger than the diameter of 50 nm of the initial tubes before GTP hydrolysis. Hence a drastic decrease in radius of curvature of the dynamin molecules corresponding to a strong constriction of the dynamin spiral, which would be necessary to produce a direct cut of the membrane tubule, is unlikely to result from GTP hydrolysis.

Therefore, we suggest that the conformational change of dynamin is manifested by an increase in pitch of the dynamin helix, whereas the radius of its cross section remains unchanged. In other words, as a result of GTP hydrolysis, the dynamin helix becomes stretched along its axis rather than constricted in its radius. Experimental evidence for a possibility of this kind of conformational change of dynamin has been reported very recently (Stowell et al., 1998). We show that such stretching of the helix produces local tightening of the lipid tubule in the regions where the membrane is not bound to dynamin. We demonstrate that this tightening results in closure of the membrane tubule, provided that the increase of the spiral pitch caused by GTP hydrolysis is sufficiently large. This closure is supposed to be the factor driving the ultimate fission of the tubule.

QUALITATIVE MODEL AND SUGGESTED SCENARIO

Major assumptions

We consider a dynamin helix coating a lipid tubule (Fig. 1). This structure is formed as a result of binding of dynamin molecules to a flat lipid bilayer, followed by their self assembly into a helix and constriction of the bilayer into a tubule inside the helix (Sweitzer and Hinshaw, 1998).

We assume the membrane to be bound to dynamin along a spiral line lying on the internal surface of the helix. This

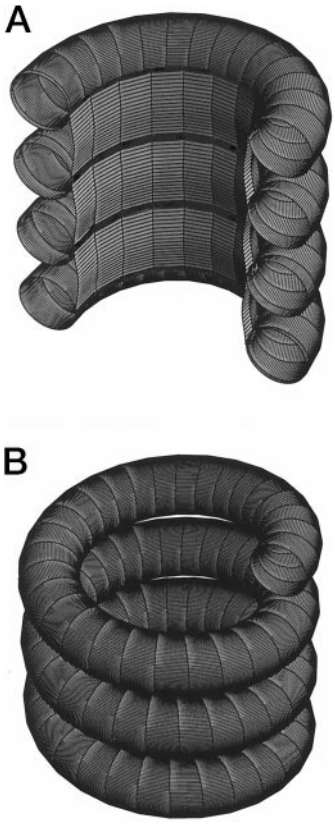

FIGURE 1 Dynamin-coated lipid tubule. (*A*) Cross section of the dynamin helix constricting a membrane tubule inside it. The line of attachment of the membrane to dynamin, called the *attachment line*, is shown by a solid line. The relative dimensions of all elements of the figure are chosen to correspond to the data by Sweitzer and Hinshaw (1998). (*B*) Dynamin helix, presented separately from the membrane.

line is named below the attachment line (Fig. 1 *A*). This binding will be assumed to persist in the course of further transformations of the system. In the points, which do not lie on the attachment line, the lipid membrane is not bound to dynamin.

We further assume that the area of the lipid bilayer constricted inside the dynamin helix is determined by the process of helix self-assembly and then kept constant in the course of all following transformations of the system. This is certainly the case for the tubes obtained by Sweitzer and Hinshaw (1998), which have no connections to any lipid vesicle and, hence, have no reservoir to exchange the lipid material with. On the other hand, this is less obvious for the neck of an endocytic bud, which is connected to the vesicle on one side and to the plasma membrane on the other. Therefore, our assumption implies that the attachment of lipid to dynamin plays the role of a barrier for lipid exchange, so that the lipid material at least in one monolayer of the neck is separated from the surrounding membranes.

We do not assume conservation of the aqueous volume inside the lipid tubule, implying that the internal aqueous solution can exchange with the outer medium. This is straightforward for the necks of endocytic vesicles, where the two ends of a short membrane tubule are open toward the internal volumes of the vesicle and the cell. The ends of the long lipid tubules of Sweitzer and Hinshaw (1998) are closed, but the membrane may be rather permeable for water, so that the aqueous exchange, although delayed in time, is supposed to proceed.

Configurational interaction and "pinchase" action

There is an interaction between the configuration of the dynamin helix and the shape of the membrane tubule. Indeed, the membrane of the tubule tends to flatten to release the elastic stresses resulting from its constriction. On the other hand, because of the binding between lipid and dynamin, such flattening cannot proceed without a related deformation of the dynamin helix producing elastic stresses in the latter. Thus the elasticities of the dynamin helix and the lipid membrane compete and determine in this way the equilibrium configuration of the whole system (Fig. 1 *A*). Any change of configuration of the helix results in a related change of the membrane shape. We will call this *configurational interaction* between the helix and the tubule. The major factors determining this interaction are 1) the permanent binding between lipid and dynamin, 2) the constant area of lipid as related to the length of the dynamin helix, and 3) the elastic properties of the membrane and the helix.

The scenario of the "pinchase" action of dynamin, we suggest, comprises the following steps:

1. Hydrolysis of bound GTP results in a change of configuration of the dynamin helix, manifested in growth of its pitch.
2. This leads to a local tightening and even local closure of the membrane tubule mediated by the configurational interaction.
3. This change of the membrane shape promotes fission of the tubule in the regions of the tightening.

To justify this scenario we 1) analyze the conformational interaction between the dynamin helix and the bilayer tubule; 2) determine a character of a conformational change of the helix, which is necessary for tightening of the tubule supporting its fission, and show that it should be a growth of the helical pitch rather than a reduction of the helical cross section; 3) show that the conclusions of the model are in reasonable agreement with the existing experimental knowledge.

MATHEMATICAL MODEL

To perform the analysis we have to express in exact terms the elastic energy of the system and the configurations of the dynamin helix and the membrane tubule.

Elasticity of the membrane

Elasticity of fluid lipid membranes is manifested by their resistance to deformations of bending and area stretching. It

is characterized by the corresponding material constants, the moduli of bending and stretching.

The stretching modulus λ of a regular membrane is rather high, $\lambda \simeq 200$ dyn/cm (Zhelev, 1998, and references therein). As a result, the lipid bilayers are practically unstretchable in the range of tensions up to ~1 dyn/cm, which a membrane can stand without rupture (Zhelev and Needham, 1993, and references therein). Thus we will assume that the area of the tubular membrane is not stretched in the course of all deformations considered.

The resistance of a lipid bilayer to bending is relatively weak (a consequence of its small thickness, ~5 nm), the bending modulus κ being about $\kappa \simeq 20kT$, where k is the Boltzmann constant and T is the absolute temperature (Helfrich, 1973). Therefore, the membranes easily undergo bending deformations, resulting in considerable changes of their shapes (Lipowsky, 1995; Seifert, 1997, and references therein). We will explicitly use this property of lipid membranes in consideration of shape changes of tubular membranes. The bending model presented and used below is due to Helfrich (1973).

The state of local bending is determined by two geometrical characteristics of the membrane surface, the two principal curvatures c_1 and c_2 (Fig. 2 *A*). Alternatively, the two combinations of these values are used, the total curvature $J = c_1 + c_2$ and the Gaussian curvature $K = c_1 \cdot c_2$. The Gaussian curvature K does not contribute to the energetics of the membrane, provided that the membrane topology does not change. Hence it is not involved in the following analysis.

The local bending energy per unit area of the membrane is given by

$$F_m = \tfrac{1}{2}\kappa \cdot (J - J_s)^2 \qquad (1)$$

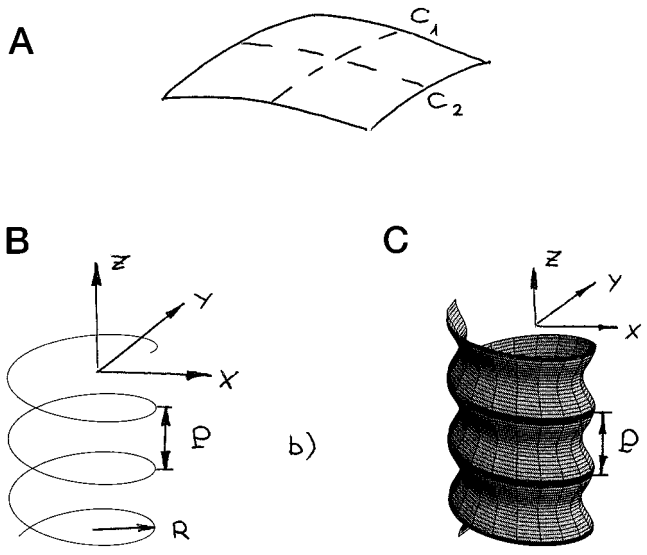

FIGURE 2 Geometry of the membrane and the helix. (*A*) Element of the membrane surface: the principal curvatures c_1 and c_2. (*B*) Attachment line of spiral form: the radius of cross section R and the pitch P. (*C*) Helicoidal tubular surface containing the attachment line, the latter shown by a solid line.

where J is the local value of the total curvature. The value J_s is called the *spontaneous curvature* of the membrane and characterizes the relaxed local shape of the membrane surface in the absence of any external forces deforming it. In the following we will assume that the spontaneous curvature of the tubular membrane vanishes, $J_s = 0$. The total bending energy of the tubule is obtained by integration of Eq. 1 over the membrane area.

Elasticity of the dynamin helix

We will describe the elasticity of the dynamin helix in a way analogous to the description of the membrane elasticity sketched above. The shape of the dynamin helix will be represented by the spiral attachment line (Fig. 2 *B*). We will assume that the helix is unstretchable, which means that the length of the line does not change in the course of all deformations of the system. The line is curved (Fig. 2 *B*), and its state of bending can be characterized by two values, the curvature c and the torsion τ (see, for example, Kreyszig, 1988), which are analogous to the two principal curvatures of a surface. These characteristics cannot be easily illustrated graphically, but in the case of a spiral line they are directly related by the expressions below to the radius R of the spiral cross section and the spiral pitch P shown in Fig. 2 *B*.

We assume a helix, which is formed spontaneously and is not subjected to any external force deforming it, to have a relaxed shape determined by the spontaneous curvature c_s and spontaneous torsion τ_s. In case the helix is deformed with respect to its spontaneous shape, its elastic energy is quadratic in deformations of the curvature and the torsion. We will present this energy per unit length of the attachment line by

$$f_h = \frac{1}{2}k_c \cdot (c - c_s)^2 + \frac{1}{2}k_\tau \cdot (\tau - \tau_s)^2 \qquad (2)$$

The values k_c and k_τ are the elastic moduli of the dynamin helix determining its resistance to the deformation of curvature and torsion, respectively.

Formalization of the effect of GTP hydrolysis

It is agreed that hydrolysis of bound GTP results in the conformational change of dynamin molecules (Sweitzer and Hinshaw, 1998; McNiven, 1998). A key assumption of the present model is that the effect of GTP hydrolysis on dynamin conformation can be cast as a change in the spontaneous characteristics c_s and τ_s of the helix.

Configurations of the helix

The attachment line is represented by the rectangular coordinates of its points $\{x, y, z\}$, determined as functions of one

variable ξ in a common form of a spiral (Kreyszig, 1988):

$$x = R \cdot \cos(\xi)$$
$$y = R \cdot \sin(\xi) \quad (3)$$
$$z = p \cdot \xi$$

where the z axis is the axis of the spiral (Fig. 2 *B*). The parameter R determines the radius of the spiral cross section perpendicular to z (Fig. 2 *B*). The parameter p, which will be called the *pitch parameter*, is related to the spiral pitch P (Fig. 2 *B*) by $P = 2\pi p$. The relationships between the curvature c and the torsion τ of the helix on one hand, and the radius R and the pitch parameter p of the helix, on the other, are given by (Kreyszig, 1988)

$$c = \frac{R}{(R^2 + p^2)}, \quad \tau = \frac{p}{(R^2 + p^2)} \quad (4)$$

$$R = \frac{c}{(c^2 + \tau^2)}, \quad p = \frac{\tau}{(c^2 + \tau^2)} \quad (5)$$

In the relaxed state, the spontaneous radius R_s and pitch parameter p_s of the helix are related to the spontaneous curvature c_s and torsion τ_s by Eq. 5.

Shape of the tubule

The surface of the tubule contains the attachment line (Eq. 3), and, hence, it has a helicoidal shape (Fig. 2 *C*), which can be presented in the form

$$x = R \cdot [1 + \epsilon(\eta)] \cdot \cos(\xi)$$
$$y = R \cdot [1 + \epsilon(\eta)] \cdot \sin(\xi) \quad (6)$$
$$z = p \cdot \xi + \eta$$

Note that, although resembling Eq. 3 for the spiral line, the expressions in Eq. 6 describe a surface. Indeed, whereas the coordinates of Eq. 3 depend on just one parameter ξ, the coordinates of Eq. 6 are functions of two parameters, ξ and η. Hence, according to the differential geometry (Vekua, 1978), Eqs. 3 and 6 determine, respectively, a line and a surface in the three-dimensional space. We have chosen the parameterizations of the attachment line (Eq. 3) and the tubular surface (Eq. 6) in such a way that the parameter ξ is common for them. As shown below, this is the most straightforward way to account for the fact that the attachment line lies on the surface. The parameter η determines the additional dimensionality of the surface (Eq. 6) compared to the line (Eq. 3). Whereas ξ changes in indefinite limits, η changes in the range $0 \le \eta \le 2\pi p$. The combination

$$r(\eta) = R \cdot [1 + \epsilon(\eta)] \quad (7)$$

represents the radius of the tubule cross section $r(\eta)$ varying along the tubular surface (Fig. 2 *C*).

The line (Eq. 3) lies on the surface (Eq. 6) in the points corresponding to $\eta = 0$ and $\eta = 2\pi p$ (Fig. 2 *C*). This means that the parameters R and p are common for Eqs. 3 and 6, whereas the function $\epsilon(\eta)$ satisfies

$$\epsilon(0) = \epsilon(2\pi p) = 0 \quad (8)$$

In addition to Eq. 8, we will assume

$$\left.\frac{d\epsilon}{d\eta}\right|_{\eta=0} = \left.\frac{d\epsilon}{d\eta}\right|_{\eta=2\pi p} = 0 \quad (9)$$

meaning that the membrane profile changes smoothly across the attachment line (Fig. 2 *C*).

In the following we will mainly be interested in the cases where the function $\epsilon(\eta)$ has negative values, meaning, according to Eq. 7, that the radius of the tubular cross section $r(\eta)$ is smaller than the radius R of the helix (everywhere except the points lying on the attachment line) and, hence, describes a tightening of the tubule. On the other hand, the absolute value of this function is not allowed to exceed one, $|\epsilon(\eta)| \le 1$, as the radius $r(\eta)$ cannot become negative. Therefore, for simplicity, we will assume $|\epsilon(\eta)| \ll 1$ and retain in major calculations (but in the Appendix) the contributions of the first order in $\epsilon(\eta)$. Extending in some cases these calculation up to $\epsilon(\eta) = 1$, we will keep in mind that the resulting conclusions can be only regarded as qualitative ones.

For the analysis below we need to know the distribution of the mean curvature across the tubular surface $J(\eta)$ determining the membrane energy (Eq. 1) and the area a of the membrane related to a unit length of the helix and conserved in the course of all deformations of the system. The geometrical calculation performed in Appendix A results in our approximations:

$$J = -\frac{1}{R}[1 - \epsilon(\eta)] + \left(1 + \frac{p^2}{R^2}\right) \cdot R \cdot \frac{d^2\epsilon}{d\eta^2} \quad (10)$$

and

$$a = \frac{R}{\sqrt{R^2 + p^2}}\left[2\pi p + \int_0^{2\pi p} \epsilon \, d\eta\right] \quad (11)$$

The complete expressions for the membrane curvature J and the area a are presented in Appendix A by Eqs. A2 and A3, respectively. Note that the value a has units of length, because it expresses the membrane area related to the unit length of the attachment line. According to Eqs. 6 and 7, the case of vanishing function ϵ corresponds to the cylindrical shape of the membrane tubule. Insertion of $\epsilon =$ into Eqs. 10 and 11 can serve to verify these expressions. We obtain, as expected, the result that the curvature of the tubule is constant along its surface and is equal to the inverse cylindrical radius $J = -1/R$; the negative sign results from the conventional definition (Vekua, 1978). The membrane area per unit length of the attachment line is equal in this case to $a = 2\pi pR/\sqrt{R^2 + p^2}$, which can easily be checked by

dividing the area of a cylinder of radius R by the length of a spiral line lying on its surface and characterized by pitch $2\pi p$.

RESULTS

Determination of equilibrium configuration

Configurational interaction is determined by the total elastic energy of the system f_t summarizing the energies of the helix f_h and the tubule f_m, so that $f_t = f_h + f_m$. All of these energies are related to the unit length of the dynamin helix.

The contribution of the helix f_h is given by Eq. 2. To find the contribution of the membrane f_m, we have to insert Eq. 10 for the curvature into the energy (Eq. 1), integrate the resulting expression over the membrane area, and relate the result to the unit length of the attachment line. A calculation presented in the Appendix results in our approximation in

$$f_m = \frac{1}{2}\,\kappa \cdot \frac{1}{R\sqrt{R^2 + p^2}} \cdot \left[2\pi p - \int_0^{2\pi p} \epsilon \, d\eta \right] \qquad (12)$$

Taking into account Eqs. 2, 4, 5, 11, and 12, the total elastic energy of the system is presented as a function of the pitch parameter p and the radius R of the dynamin helix by

$$f_t = \frac{1}{2}\,k_c\left[\frac{R}{(R^2 + p^2)} - c_s\right]^2 + \frac{1}{2}\,k_\tau\left[\frac{p}{(R^2 + p^2)} - \tau_s\right]^2 + \frac{1}{2}\,\kappa \cdot \frac{1}{R\sqrt{R^2 + p^2}} \cdot \left[4\pi p - \frac{\sqrt{R^2 + p^2} \cdot a}{R}\right] \qquad (13)$$

Minimization of Eq. 13 results in the values of p^* and R^* determining the equilibrium configuration of the helix.

An exact way to obtain the corresponding equilibrium shape of the membrane tubule (Eq. 6) would be to find such a function $\epsilon(\eta)$, which minimizes the energy f_m at the fixed values of parameters p^* and R^* and, at the same time, satisfies the constraint (Eq. 11) of constant area a along with Eqs. 8 and 9. For qualitative purposes of this study, we chose a simple but approximate way to determine the membrane shape. We assume $\epsilon(\eta)$ to have a specific form, justified in Appendix A:

$$\epsilon(\eta) = u_0 \cdot \left[1 - \cos\left(\frac{\eta}{p}\right)\right] \qquad (14)$$

which satisfies the requirements of Eqs. 8 and 9, so that the membrane shape is now determined by the unique parameter u_0.

Substitution of Eq. 14 into 11 gives

$$u_0 = a \cdot \frac{\sqrt{R^{*2} + p^{*2}}}{2\pi p^* R^*} - 1 \qquad (15)$$

The sign of u_0 determines the sign of the whole function $\epsilon(\eta)$ (Eq. 14) and, thus, the qualitative character of the membrane shape (Eqs. 6 and 7). At $u_0 = 0$ the tubule is a regular cylinder containing the attachment line (Fig. 3 *A*). At negative $u_0 < 0$, the tubule is tightened with respect to the helix everywhere but the points on the attachment line (Fig. 3 *B*), whereas in the opposite case of $u_0 > 0$ the tubule tends to swell compared to the helix (Fig. 3 *C*).

We will perform the further analysis in two steps. First, we will assume that the helix is much more rigid than the membrane. This will allow us to see the major features of the model. After that we will analyze the effects related to the nonvanishing rigidity of the membrane.

Rigid helix and flexible membrane: tightening of the membrane tube

The rigidities of the helix and the membrane can be compared in terms of their elastic moduli brought to the same units. The elastic moduli of the helix, k_c and k_τ, are measured in erg · cm, and the unit of the bending modulus of membrane κ is the erg. A simple analysis shows that the convenient values to compare are k_c and k_τ, on one hand, and $\kappa \cdot R_s$, on the other, where R_s is the radius of the helix cross section in the spontaneous state.

The helix is much more rigid than the membrane if

$$\frac{\kappa \cdot R_s}{k_c} \ll 1, \quad \frac{\kappa \cdot R_s}{k_\tau} \ll 1 \qquad (16)$$

Inspection of the total elastic energy (Eq. 13) shows that in the case of Eq. 16 the membrane influences only very slightly the configuration of the helix. This case seems to be rather realistic, as the experiments show that the geometric parameters of the dynamin helices assembled in aqueous solution in the absence of lipid (Hinshaw and Schmid, 1995; Carr and Hinshaw, 1997) are very similar to those of the helices constricting the lipid membranes inside them (Sweitzer and Hinshaw, 1998). Thus a membrane tubule practically does not change the configuration of a dynamin helix.

In zero-order approximation in the ratios (Eq. 16), we completely neglect the rigidity of the membrane as compared with the rigidity of the helix, which means that we drop in Eq. 13 the contribution of the membrane proportional to κ and minimize the energy, accounting only for the first two contributions related to the helix elasticities k_τ and k_c.

In this approximation, the equilibrium configuration of the spiral is its spontaneous configuration,

$$R^* = R_s, \quad p^* = p_s \qquad (17)$$

The parameter u_0 (Eq. 15) determining the corresponding shape of the membrane tubule is expressed through the spontaneous characteristics of the helix by

$$u_0 = a \cdot \frac{\sqrt{R_s^2 + p_s^2}}{2\pi p_s R_s} - 1 \qquad (18)$$

Inserting Eqs. 17 and 18 into Eq. 14 and then into Eq. 6, we obtain the shape of the tubule. The case of a rigid helix and a flexible membrane corresponds to "one-way" configura-

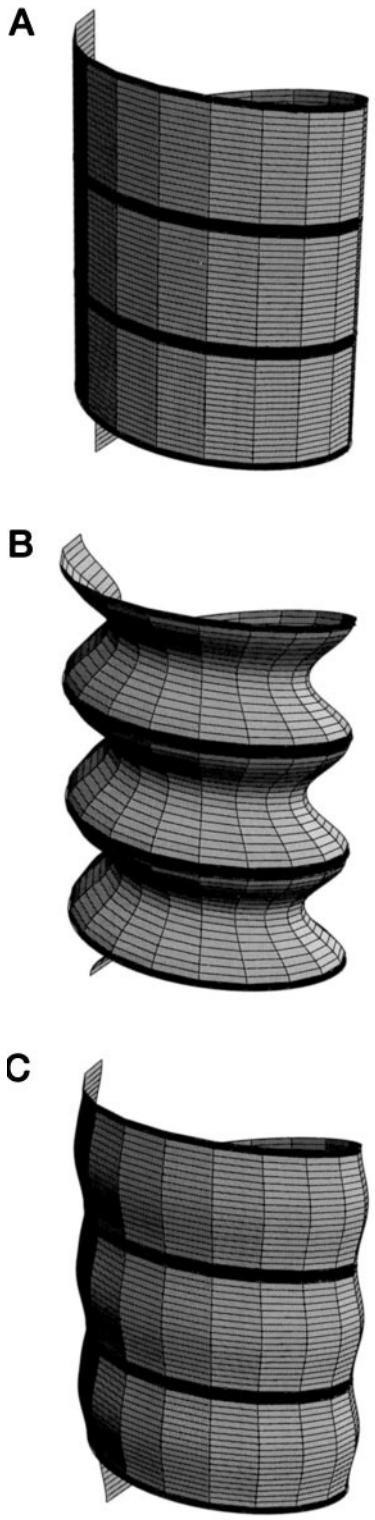

FIGURE 3 The shape of the tubular surface at different u_0 (Eq. 14). The attachment line is shown by the thick solid line on the surface. (*A*) $u_0 = 0$ corresponding to $a = 13.1$ nm, $R^* = 15$ nm, and $p^* = 2.1$ nm. (*B*) Tightening of the tubule at $u_0 < 0$, corresponding to $a = 13.1$ nm, $R^* = 15$ nm, and $p^* = 2.5$ nm. (*C*) Swelling of the tubule at $u_0 > 0$, corresponding to $a = 13.1$ nm, $R^* = 7$ nm, and $p^* = 2.1$ nm.

tional interaction, meaning that this interaction drastically influences the shape of the membrane tubule, whereas the helix remains in its undisturbed spontaneous configuration.

To proceed, we estimate the parameters of the helix, R_s and p_s, using the data by Sweitzer and Hinshaw (1998). According to these measurements, the radius is about $R_s \simeq 15$ nm, and the pitch of the helix is $P_s = 2\pi p_s \simeq 13$ nm. Thus $p_s^2/R_s^2 \simeq 0.02$, and we can consider it to be a small parameter. Expanding Eq. 18 in p_s^2/R_s^2 and retaining the first nonvanishing order, we obtain

$$u_0 = \frac{a}{2\pi p_s}\left[1 + \frac{1}{2}\frac{p_s^2}{R_s^2}\right] - 1 \tag{19}$$

Equation 19 shows that tightening of the tube corresponding to negative u_0 is driven by growth of the helical pitch parameter p_s, as illustrated in Fig. 3 *B*. In contrast, constriction of the helical radius R_s, previously suggested as a factor supporting the fission of the tubule, promotes, although weakly, swelling of the tube with respect to the helix (Fig. 3 *C*). Because we are interested in the tightening of the tube rather than in its swelling, we will suppose that the result of GTP hydrolysis is an increase in the pitch parameter p_s, while the radius R_s of the helix remains unchanged.

Fig. 4, *A–E*, illustrates the evolution of the helix and the attached membrane tube in the course of growth of the helical pitch parameter p_s. We assume, based on the electron micrographs by Sweitzer and Hinshaw (1998), that before GTP hydrolysis the initial configuration of the dynamin helix is characterized by the pitch parameter $p_s^0 = 13.2$ nm/$2\pi = 2.1$ nm and radius $R_s = 15$ nm, whereas the tubular membrane has a shape close to a regular cylinder, which means that its area per unit length of the helix has the value $a = 2\pi p_s^0 R_s/\sqrt{p_s^{02} + R_s^2} \simeq 13$ nm. This initial state is illustrated in Fig. 4 *A*.

In the course of GTP hydrolysis, a and R_s remain unchanged, while p_s grows. The configuration of the system corresponding to the pitch parameter p_s adopting the values 3, 4, and 4.5 nm are presented in Fig. 4, *B–D*, respectively. One can see that the membrane tube tightens in the middle of each turn of the helicoidal surface. When the pitch parameter reaches a value close to $p_s \simeq 4.5$ nm, the membrane tube becomes closed (Fig. 4 *D*). Further increase of the pitch leads in our presentation to nonphysical self-intersection of the membrane (Fig. 4 *E*), which means that in reality the membrane becomes more and more tightly closed and its shape is no longer described by our equations.

We suggest that the tightening of the membrane tubule up to its closure is the condition supporting the fission of the tubule.

Effects of rigidity of the membrane: reduction of the helix diameter

In the approximation above, neglecting completely the rigidity of the membrane compared to that of the helix, we demonstrated the major effect of our model: tightening of

the tubule by growing helical pitch. We have also shown that the decrease in the spontaneous radius R_s of the helix assumed in the previous models results in swelling of the tubule with respect to the helix (Fig. 3 *C*) rather than in its tightening. In other words, reduction of R_s leads to a tendency opposite that supporting fission of the tubule.

On the other hand, provided that the structures seen in the micrographs of Sweitzer and Hinshaw (1998) as constricted and twisted helices are indeed the precursors of the vesicles, the dynamin helices do undergo a ~20% reduction of their external diameter before fission of the tubes.

We show now that a nonvanishing rigidity of the membrane of the tubule can account for a tendency of the helix diameter to reduce despite constant R_s.

We minimize the energy (Eq. 13) accounting for the first nonvanishing order in the small parameters $\kappa \cdot R_s/k_c$ and $\kappa \cdot R_s/k_\tau$. The resulting expressions for the equilibrium geometric parameters of the helix R^* and p^*, using a notation $\lambda = p_s/R_s$, have the form

$$R^* = R_s \cdot \left\{ 1 - \frac{\kappa \cdot R_s}{k_c} \cdot 2\pi(1-\lambda^2)\left[\frac{\lambda^3}{(1+\lambda^2)^{1/2}} + \frac{1}{2\pi}(1-\lambda^2)\frac{a}{R_s} \right] + \frac{\kappa \cdot R_s}{k_\tau} \cdot 4\pi\lambda \left[\frac{1+3\lambda^2+2\lambda^4}{(1+\lambda^2)^{3/2}} - \frac{1}{\pi}\lambda\frac{a}{R_s} \right] \right\} \quad (20)$$

$$p^* = p_s \cdot \left\{ 1 - \frac{\kappa \cdot R_s}{k_c} \cdot 4\pi \left[\frac{\lambda^3}{(1+\lambda^2)^{1/2}} + \frac{1}{2\pi}(1-\lambda^2)\frac{a}{R_s} \right] - \frac{\kappa \cdot R_s}{k_\tau} \cdot 2\pi \frac{1-\lambda^2}{\lambda} \left[\frac{1+3\lambda^2+2\lambda^4}{(1+\lambda^2)^{3/2}} - \frac{1}{\pi}\lambda\frac{a}{R_s} \right] \right\} \quad (21)$$

The expressions 20 and 21 illustrate the contribution of the membrane rigidity κ to the configurational interaction. The equilibrium parameters of the helix, R^* and p^*, deviate, although slightly, from the spontaneous parameters, R_s and p_s, this deviation depending on the values of the latter.

We concentrate on the change in the equilibrium radius of the helix R^* resulting from the growth of the spontaneous pitch parameter p_s. Analysis of Eq. 20 shows that R^* can decrease or increase with p_s, depending on ratios $\kappa \cdot R_s/k_c$ and $\kappa \cdot R_s/k_\tau$. Specifically, the second contribution to Eq. 20, proportional to $\kappa \cdot R_s/k_\tau$, supports an increase of the radius R^*, whereas the first contribution, proportional to $\kappa \cdot R_s/k_c$, determines the reduction of R^*. Therefore, to explain the experimentally observed decrease in the radius of the helix R^*, we have to assume that $\kappa \cdot R_s/k_\tau \ll \kappa \cdot R_s/k_c$. In other words, the modulus of torsion of the helix has to be much larger than its modulus of bending, $k_\tau \gg k_c$. The decreasing behavior of the radius of the helix R^* at growing pitch parameter p_s is illustrated in Fig. 5 for a tentative value of $\kappa \cdot R_s/k_c = 0.1$ and a negligible $\kappa \cdot R_s/k_\tau \simeq 0$. The changes in R^* shown in Fig. 5 are smaller than those observed experimentally. This quantitative disagreement may be related to the strong approximations made in our analysis for the sake of its simplification. It is important, however, that our model provides a qualitative explanation of the constriction of the helix, which occurs along with the tightening of the membrane tubule and results from configurational interaction between the helix and the tubular membrane.

DISCUSSION AND CONCLUSIONS

This study addresses a mechanism of fission of a membrane tubule constricted inside a dynamin helix. The fission is induced by a conformational change of dynamin resulting from hydrolysis of bound GTP.

Previous ideas on physical factors driving this process (Sweitzer and Hinshaw, 1998; McNiven, 1998) are based on the experimental observation that, although most tubules are transformed by GTP hydrolysis into vesicles, several tubes still remain in the system but become constricted with respect to their initial shape. The diameter of the initial tubes is close to 50 nm, whereas the diameter of the tubes left after GTP hydrolysis is reduced to 40 nm. These transformed tubes are supposed to be precursors of the vesicles. Thus it was suggested that the conformational change of dynamin induced by GTP hydrolysis leads to a reduction in the diameter of the dynamin helix. Although this reduction is rather modest, constituting 20–30% of the initial diameter, it may be sufficient for the membrane tubule constricted inside the helix to lose its stability and undergo fission (Sweitzer and Hinshaw, 1998; McNiven, 1998).

Our analysis does not confirm such a mechanism of fission. Indeed, as follows from Eqs. 18 and 19 and illustrated in Fig. 3 *C*, compression of the membrane tubule in the points contacting the dynamin helix results in its swelling everywhere else. Such a tendency is opposite that required for the loss of stability leading to fission of the tube. Let us emphasize that the origin of this result is a purely geometrical one related to the constancy of the membrane area restricted inside the dynamin helix.

Another possibility mentioned previously is a direct slicing of a lipid tube by dynamin (McNiven, 1998), along the line of its attachment to the helix. This, however, seems to require a drastic reduction of the diameter of the dynamin helix to a value of a few nanometers, constituting the thickness of a lipid membrane. There is no experimental evidence for such a strong change in dynamin shape. Indeed, as just mentioned, the constriction of the remaining helices is only 20–30%, which is not sufficient for slicing. One can argue that these tubes do not represent the final state of dynamin after GTP hydrolysis, in which the helices are constricted to very small radii but cannot be observed because of their immediate transformation into vesicles. In such a case one would expect the observable final structures to have dimensions corresponding to very small radii of curvature of the dynamin molecules. Contrary to this expectation, the dynamin-coated vesicles, which are supposed to represent the final state of the system, have diameters of

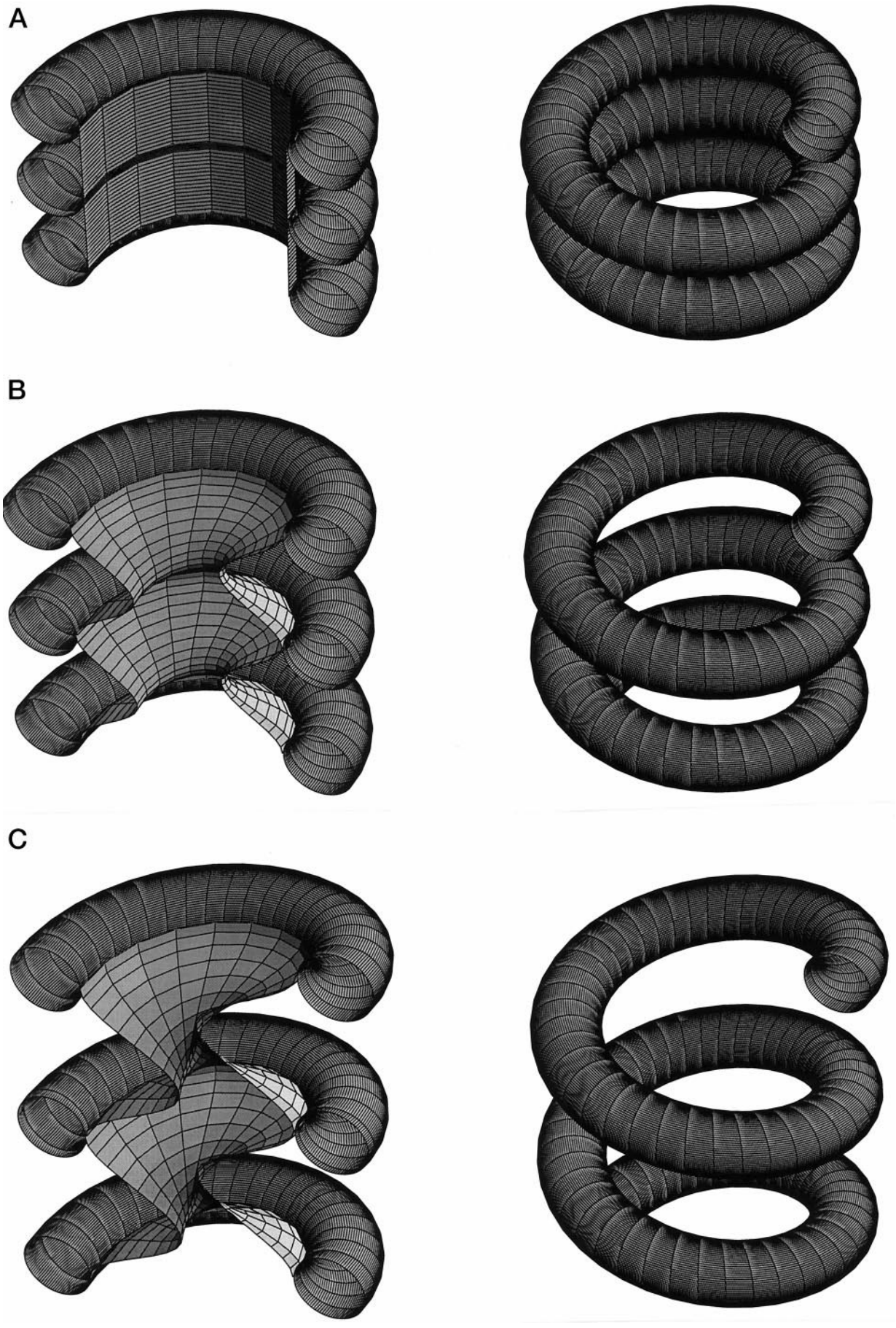
A
B
C

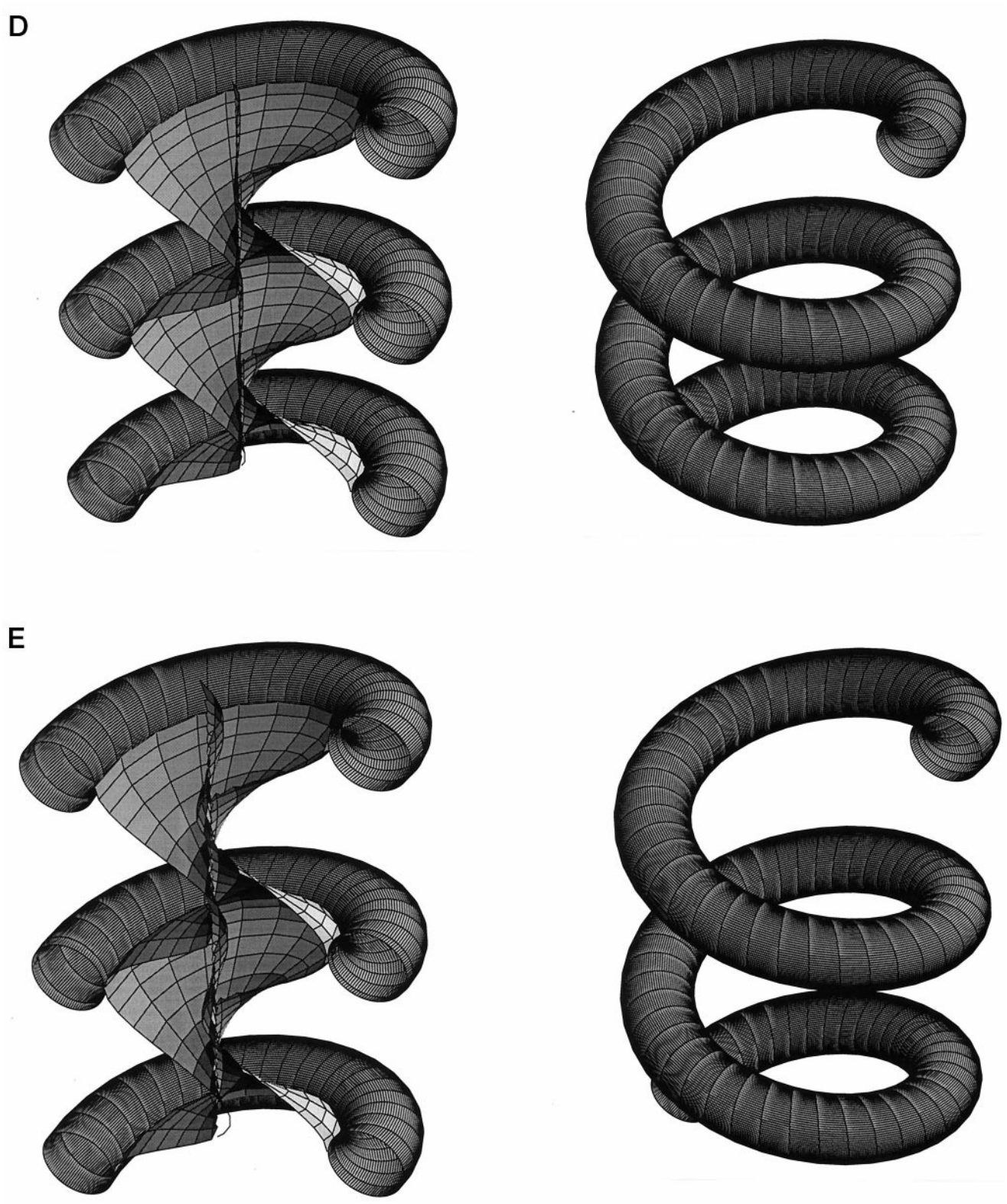

FIGURE 4 Evolution of the shape of the membrane tubule in the course of growth of the spontaneous pitch parameter p_s of the dynamin helix at constant $R_s = 15$ nm and $a = 13.1$ nm. (*A*) $p_s = 2.1$ nm. (*B*) $p_s = 3$ nm. (*C*) $p_s = 4$ nm. (*D*) $p_s = 4.5$ nm. (*E*) $p_s = 5.0$ nm. On the left-hand side of each figure the whole system consisting of the helix and the attached membrane is presented, and on the right-hand side the dynamin helix is shown separately from the membrane to illustrate the changes in its spontaneous geometrical characteristics.

~60 nm (Sweitzer and Hinshaw, 1998), which is even slightly larger than the diameter of the initial dynamin-coated tubules. This means that the dynamin molecules may even tend to unbend as a result of GTP hydrolysis.

Therefore, we propose an alternative mechanism for fission of the tubule. The most important features of our model are the following. We assume that

1. The lipid bilayer is bound to the dynamin helix only along a spiral attachment line rather than across the whole area of the membrane, but this binding is stable.

2. The area of the lipid bilayer per unit length of the attachment line is conserved during all transformations.

We show that

1. The conformational change in dynamin induced by GTP hydrolysis has to consists in increase of the pitch of the dynamin helix, and not in compression of the helix. A lengthiness of the dynamin spirals resulting from phosphorylation of GTP has been reported very recently (Stowell et al., 1998), supporting this prediction of our model.

Our analysis shows that the growth of the helical pitch results in local tightening and closure of the attached membrane tubule (Fig. 4), i.e., fulfilling the task of a "pinchase" machine.

It is important to emphasize that within our model we do not treat the last stage of fission, resulting in separation of the tube into vesicles. Indeed, the local tightening of the tubule provides the conditions supporting the fission. However, the ultimate fission requires an additional structural rearrangement of the membrane in the region of closure of the tubule. It may be a transient rupture of the membrane and its immediate reconstitution into the new vesicular topology. This stage and the required conditions and properties of the lipid bilayer remain to be analyzed.

The idea of our model is close to those treating the phenomena of fission of membrane tubules by lateral tension. One example is the mechanism of fission of a lipid membrane tube formed between two reservoirs of lipid solution in organic solvent and, hence, subjected to lateral tension (Melikyan et al., 1984). Another, similar phenomenon is pearling instability of long cylindrical lipid vesicles, in which lateral tension is induced by laser tweezers (Bar-Ziv et al., 1998, and references therein). A common feature of these phenomena is that a lateral tension in a cylindrical membrane can result in a dramatic shape change of the membrane, resulting in its collapse. In the present model an effective lateral tension in the lipid tubule is produced by the attached dynamin helix in the course of conformational change of the latter induced by GTP hydrolysis. Indeed, growth of the pitch can be seen as stretching of the helix along its axis, producing a tension in the bound membrane. This tension is then compensated for by tightening of the membrane tubule and, hence, serves as a driving force for the shape transformation of the membrane.

In addition to the suggestion of a specific mechanism for the major phenomenon of fission of a membrane tubule (Fig. 4), our model proposes an explanation for a tendency of the dynamin helices to be compressed to some extent before undergoing fission, as illustrated in Fig. 5. The driving force for this trend is interaction between the membrane shape and the conformation of the helix. We show that for this explanation to be valid, the helix has to be much more rigid with respect to torsion τ than it is with respect to curvature c, meaning that $k_\tau \gg k_c$. We do not have any data that we can use to estimate the elastic moduli of the helix and to verify this conclusion. However, it has to be stressed again that the reduction of the diameter of the helix obtained

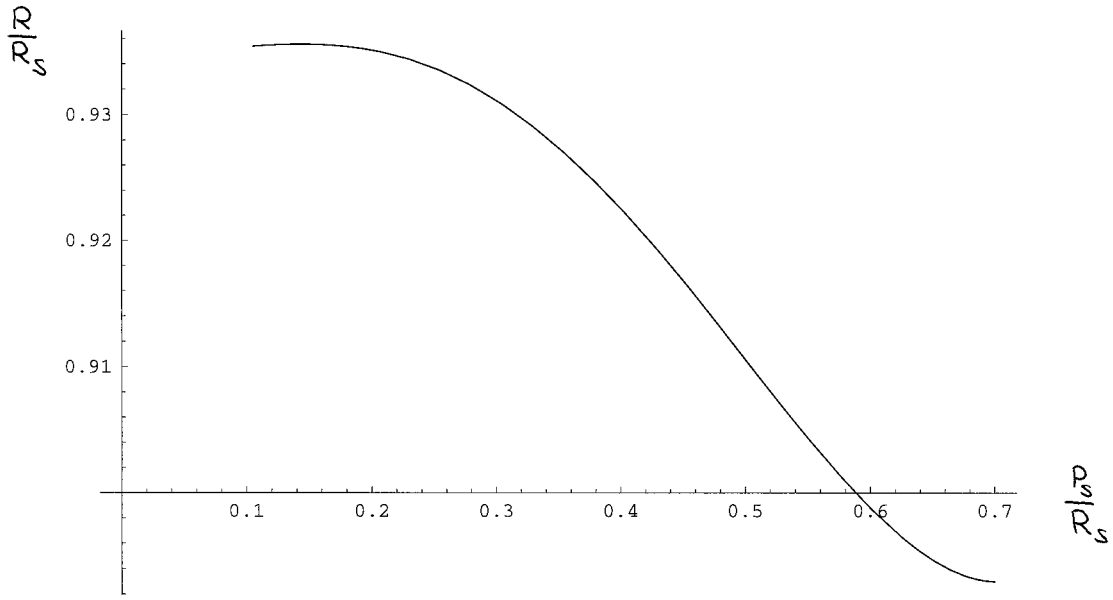

FIGURE 5 Dependence of the radius of the dynamin helix on its spontaneous pitch parameter p_s at $R_s = 20$ nm, $a = 13.1$ nm, $\kappa \cdot R_s/k_c = 0.1$, and $\kappa \cdot R_s/k_\tau = 0$.

by our simplified calculations is less than 20–30% observed (Sweitzer and Hinshaw, 1998). A reason for this disagreement may be the strong approximations of our treatment. Another possibility is that the constricted tubes remaining after GTP hydrolysis are not precursors of the vesicle, and our model does not describe them.

APPENDIX

In this section we present additional details on the geometrical characteristics of the tubular surface, calculate the membrane area per unit length of the attachment line a, and, finally, determine the bending energy of the membrane f_m. In contrast to the main presentation, in the calculations of this section we retain the contributions up to the second order in $\epsilon(\eta)$ and justify the approximative expression for the membrane shape (Eq. 14) used in the main part.

Geometrical calculation performed by means of the theory of surfaces (Vekua, 1978) and based on the presentation (Eq. 6) of the membrane shape and (Eq. 3) of the attachment line results in the expression for an element of the surface area da related to the unit length of the attachment line:

$$\mathrm{d}a = \frac{R}{\sqrt{R^2 + p^2}}\left[1 + \epsilon + \frac{1}{2}\left(1 + \frac{p^2}{R^2}\right)R^2\epsilon'^2\right]\mathrm{d}\eta \tag{A1}$$

and for a local value of the total curvature of the surface:

$$J = -\frac{1}{R}(1 - \epsilon) + \left(1 + \frac{p^2}{R^2}\right)R\epsilon'' - \frac{1}{R}\epsilon^2 + \frac{1}{2}\left(1 - \frac{p^2}{R^2}\right)R\epsilon'^2 - 2\frac{p^2}{R}\epsilon\epsilon'' \tag{A2}$$

where ϵ' and ϵ'' are the first and second derivatives of the function $\epsilon(\eta)$.

The total area a of the membrane per unit length of the attachment line is

$$a = \int_0^{2\pi p}\mathrm{d}a = \frac{R}{\sqrt{R^2 + p^2}} \cdot \left[2\pi p + \int_0^{2\pi p}\epsilon\,\mathrm{d}\eta + \frac{1}{2}\left(1 + \frac{p^2}{R^2}\right)R^2\int_0^{2\pi p}\epsilon'^2\mathrm{d}\eta\right] \tag{A3}$$

The total bending energy of the membrane per unit length of the attachment line is

$$f_m = \int_0^{2\pi p}J^2\mathrm{d}a = \frac{1}{2}\kappa\frac{1}{R\sqrt{R^2 + p^2}}\left[2\pi p - \int_0^{2\pi p}\epsilon\,\mathrm{d}\eta + \int_0^{2\pi p}\epsilon^2\mathrm{d}\eta + (R^2 + p^2)^2\int_0^{2\pi p}\epsilon''^2\mathrm{d}\eta - \frac{1}{2}(R^2 + 5p^2)\int_0^{2\pi p}\epsilon'^2\mathrm{d}\eta\right] \tag{A4}$$

The function $\epsilon(\eta)$ determining the shape of the tubule can be presented as a Fourier expansion, which, taking into account the boundary condition (Eq. 9), has the form

$$\epsilon(\eta) = u_0 + \sum_1^\infty u_k\cos\left(k\frac{\eta}{p}\right) \tag{A5}$$

where the boundary condition of Eq. 8 is satisfied if

$$u_0 + \sum_1^\infty u_k = 0 \tag{A6}$$

Inserting Eq. A5 into Eq. A4 and performing integration, we obtain for the energy

$$f_m = \frac{1}{2}\kappa\frac{2\pi p}{R\sqrt{R^2 + p^2}}\left\{1 - u_0 + u_0^2 + \frac{1}{2}\sum_1^\infty u_k^2\left[\left(\frac{R^2}{p^2} + 1\right)^2k^4 - \frac{1}{2}\left(\frac{R^2}{p^2} + 5\right)^2k^2 + 1\right]\right\} \tag{A7}$$

Instead of minimizing the energy f_m with respect to the set of coefficients $\{u_k\}$, taking into account the condition of Eq. A6, we approximate the shape by just one mode of the Fourier expansion:

$$\epsilon(\eta) = u_0 + u_k\cos\left(k\frac{\eta}{p}\right) \tag{A8}$$

Inspection of Eq. A7, taking into account that $R^2/p^2 \gg 1$, shows that the mode of the minimal energy is that of $k = 1$. Hence we obtain, accounting for Eq. A6, that in our approximation the shape of the membrane tubule is determined by

$$\epsilon(\eta) = u_0\left[1 - \cos\left(\frac{\eta}{p}\right)\right] \tag{A9}$$

I thank Leonid Chernomordik for attracting my attention to the field of dynamin.

REFERENCES

Bar-Ziv, R., E. Moses, and P. Nelson. 1998. Dynamic excitations induced by optical tweezers. *Biophys. J.* 75:294–320.

Carr, J. F., and J. E. Hinshaw. 1997. Dynamin assembles into spirals under physiological salt conditions upon the addition of GDP and γ-phosphate analogues. *J. Biol. Chem.* 272:28030–28035.

Helfrich, W. 1973. Elastic properties of lipid bilayers: theory and possible experiments. *Z. Naturforsch.* 28c:693–703.

Henley, J. R., E. W. A. Krueger, B. J. Oswald, and M. A. McNiven. 1998. Dynamin-mediated internalization of calveolae. *J. Cell. Biol.* 141:85–99.

Hinshaw, J. E., and S. L. Schmid. 1995. Dynamin self-assembles into rings suggesting a mechanism for coated vesicle budding. *Nature.* 374: 190–192.

Jones, S. M., K. E. Howell, J. R. Henley, H. Cao, and M. A. McNiven. 1998. Role of dynamin in the formation of transport vesicles from the trans-Golgi network. *Science.* 279:573–577.

Kirchhausen, T. 1998. Vesicle formation: dynamic dynamin lives up to its name. *Curr. Biol.* 8:R792–R794.

Kosaka, T., and K. Ikeda. 1983. Possible temperature-dependent blockage of synaptic vesicle recycling induced by a single gene mutation in *Drosophila. J. Neurobiol.* 14:207–225.

Kreyszig, E. 1988. Advanced Engineering Mathematics. John Wiley and Sons, New York.

Lipowsky, R. 1995. The morphology of lipid membranes. *Curr. Opin. Struct. Biol.* 5:531–540.

Melikyan, G. B., M. M. Kozlov, L. V. Chernomordik, and V. S. Markin. 1984. Fission of bilayer lipid tube. *Biochim. Biophys. Acta.* 776: 169–175.

McNiven, M. A. 1998. Dynamin: a molecular motor with pinchase action. *Cell.* 94:151–154.

Oh, P., D. P. McIntosh, and J. E. Schnitzer. 1998. Dynamin at the neck of calveolae mediates their budding to form transport vesicles by GTP-driven fission from the plasma membrane. *J. Cell. Biol.* 141:101–114.

Schmid, S. L., M. A. McNiven, and P. De Camilli. 1998. Dynamin and its partners: a progress report. *Curr. Opin. Cell Biol.* 10:504–512.

Seifert, U. 1997. Configurations of fluid membranes and vesicles. *Adv. Phys.* 46:13–137.

Stowell, M. H. B., P. Wigge, B. Marks, and H. T. McMahon. 1998. Nucleotide dependent structural changes in dynamin: evidence for a mechanochemical molecular spring. *Mol. Biol. Cell.* 9:195a.

Sweitzer, S. R., and J. E. Hinshaw. 1998. Dynamin undergoes a GTP-dependent conformational change causing vesiculation. *Cell.* 93: 1021–1029.

Takei, K., V. Haucke, V. Slepnev, K. Farsad, M. Salazar, H. Chen, and P. De Camilli. 1998. Generation of coated intermediates of clathrin-mediated endocytosis on protein-free liposomes. *Cell.* 94:131–141.

Takei, K., P. S. McPherson, S. L. Schmid, and P. De Camilli. 1995. Tubular membrane invaginations coated by dynamin rings are induced by GTPγS in nerve terminals. *Nature.* 374:186–190.

Zhelev, D. V. 1998. Material property characteristics for lipid bilayers containing lysolipid. *Biophys. J.* 75:321–330.

Zhelev, D. V., and D. Needham. 1993. Tension stabilized pores in giant vesicles: determination of pore size and pore line tension. *Biochim. Biophys. Acta.* 1147:89–104.

Urrutia, R., J. R. Henley, T. Cook, and M. A. McNiven. 1997. The dynamins: redundant or distinct functions for an expanding family of related GTPases? *Proc. Natl. Acad. Sci. USA.* 94:377–384.

Vekua, I. N. 1978. Introduction to Tensor Analysis and Theory of Covariants. Moscow, Nauka.

Warnock, D. E., and S. L. Schmid. 1996. Dynamin GTPase, a force-generating molecular switch. *BioEssays.* 18:885–893.